Genetic investigation of purine nucleotide imbalance in Saccharomyces cerevisiae

Christelle Saint-Marc, Johanna Ceschin, Benoît Pinson, Claire Almyre, Bertrand Daignan-Fornier

▶ **To cite this version:**

Christelle Saint-Marc, Johanna Ceschin, Benoît Pinson, Claire Almyre, Bertrand Daignan-Fornier. Genetic investigation of purine nucleotide imbalance in Saccharomyces cerevisiae. Current Genetics, 2020, 66 (6), pp.1163-1177. 10.1007/s00294-020-01101-y . hal-03379696

HAL Id: hal-03379696
https://hal.science/hal-03379696

Submitted on 15 Oct 2021

HAL is a multi-disciplinary open access archive for the deposit and dissemination of scientific research documents, whether they are published or not. The documents may come from teaching and research institutions in France or abroad, or from public or private research centers.

L'archive ouverte pluridisciplinaire **HAL**, est destinée au dépôt et à la diffusion de documents scientifiques de niveau recherche, publiés ou non, émanant des établissements d'enseignement et de recherche français ou étrangers, des laboratoires publics ou privés.

Click here to access/download;Manuscript;Saint-Marc et al. revised.docx

Click here to view linked References

Genetic investigation of purine nucleotide imbalance in *Saccharomyces cerevisiae*

Christelle Saint-Marc [1,2,3], Johanna Ceschin[1,2,3], Claire Almyre[1,2], Benoît Pinson [1,2], Bertrand Daignan-Fornier [1,2,*]

[1] IBGC, Université de Bordeaux UMR 5095, Bordeaux, France;

[2] Centre National de la Recherche Scientifique IBGC UMR 5095, Bordeaux, France

[3] These authors contributed equally to the work

*corresponding author

Christelle Saint-Marc[1,2] 0000-0001-9537-1848

Johanna Ceschin[1,2] 0000-0001-7771-531X

Bertrand Daignan-Fornier [1,2,*] 0000-0003-2352-9700

Benoît Pinson [1,2] 0000-0003-2936-9058

Keywords

Yeast metabolism, AMP deaminase, adenine deaminase, GTP, amino acid transport

Declarations

Funding

This work was supported by CNRS and Université de Bordeaux

Conflicts of interest/Competing interests

The authors declare no conflict of interest

Ethics approval

Not Applicable

Consent to participate

Not Applicable

Consent for publication

Not Applicable

Availability of data and material

Not applicable

Code availability

Not applicable

Authors' contributions Conceptualization: Daignan-Fornier; Methodology: Saint-Marc, Ceschin, Almyre, Pinson; Formal analysis and investigation: Saint-Marc, Ceschin, Almyre, Pinson; Writing - original draft preparation: Daignan-Fornier, Pinson; Writing - review and editing: Daignan-Fornier, Pinson; Funding acquisition: Daignan-Fornier; Supervision: Daignan-Fornier

Abstract

Because metabolism is a complex balanced process involving multiple enzymes, understanding how organisms compensate for transient or permanent metabolic imbalance is a challenging task that can be more easily achieved in simpler unicellular organisms. The metabolic balance results from the combination of individual enzymatic properties, regulation of enzyme abundance, but also from the architecture of the metabolic network offering multiple interconversion alternatives. Although metabolic networks are generally highly resilient to perturbations, metabolic imbalance resulting from enzymatic defect and specific environmental conditions can be designed experimentally and studied. Starting with a double *amd1 aah1* mutant that severely and conditionally affects yeast growth, we carefully characterized the metabolic shuffle associated with this defect. We established that the GTP decrease resulting in an adenylic/guanylic nucleotide imbalance was responsible for the growth defect. Identification of several gene dosage suppressors revealed that *TAT1*, encoding an amino acid transporter, is a robust suppressor of the *amd1 aah1* growth defect. We show that *TAT1* suppression occurs through replenishment of the GTP pool in a process requiring the histidine biosynthesis pathway. Importantly, we establish that a *tat1* mutant exhibits synthetic-sickness when combined with an *amd1* mutant and that both components of this synthetic phenotype can be suppressed by specific gene dosage suppressors. Together our data point to a strong phenotypic connection between amino acid uptake and GTP synthesis, a connection that could open perspectives for future treatment of related human defects, previously reported as etiologically highly conserved.

Introduction

Metabolism is the highly integrated process of chemical interconversion in living organisms. It involves multiple enzymes organized in interconnected pathways. Although metabolic enzymes are generally highly specific and involved in a single pathway, mutations affecting metabolic enzymes can have multiple effects and result in complex phenotypes. Indeed, a simple block in a metabolic pathway, due to the lack of an enzyme activity, can have several effects such as, shortage of the product, accumulation of the substrate and/or imbalance between metabolites. All three features can contribute to the phenotype independently, additively or cooperatively and it is difficult to appraise their relative contribution which can vary in different tissues or during development (Daignan-Fornier and Pinson, 2019). The use of simpler organisms to get a primary view of the metabolic consequences of the dysfunction has proved to be valuable, as for example in the case of AMP deaminase, which catalyzes synthesis of IMP from AMP and hence contributes to the Adenylic/Guanylic nucleotides balance (Fig. 1). The yeast *amd1* mutant, lacking AMP deaminase, accumulates AMP the substrate of the reaction and its adenylic nucleotides derivatives (AXP), while it has low intracellular guanylic nucleotides (GXP) which are the physiological "end products" of the reaction (Saint-Marc et al., 2009). Addition of exogenous adenine to the growth medium is critical for the purine nucleotide imbalance and the growth defect associated with the *amd1* mutation (Saint-Marc et al., 2009). Strikingly, a similar purine nucleotide imbalance, dependent on adenylic precursors, was reported for *AMPD2* deficiency associated with a rare neurodegenerative disorder, pontocerebellar hypoplasia, in humans (Akizu et al., 2013). This remarkable conservation of a complex phenotype between yeast and human prompted us to take further advantage of yeast genetics to identify additional factors affecting the growth defect of the *amd1* mutant. In this work, we characterize mutations that modulate the phenotype of the *amd1* mutant and gene dosage suppressors that alleviate the growth defect associated with purine nucleotide imbalance in yeast.

These results revealed that, while the nucleotide imbalance due to the *amd1* mutation can be corrected through different means, no suppressors of effects downstream of the imbalance itself have been identified, hence indicating that this nucleotide imbalance most probably affects multiple physiological features and cannot easily be phenotypically circumvented.

Materials and Methods

Yeast media

SD is a synthetic minimal medium containing 0.5 % ammonium sulfate, 0.17 % yeast nitrogen base without amino acids and ammonium sulfate (BD-Difco; Franklin Lakes, NJ, USA) and 2 % glucose supplemented or not with adenine (0.3 mM) and/or histidine (0.09 mM) or uracil (0.3 mM; SDU). SDcasaW is SD medium supplemented with 0.2% casamino acids ((#A1404HA; Biokar/Solabia group; Pantin, France; this amino-acids mixture includes histidine at a final concentration of 0.3 mM in the medium) and tryptophan (0.2 mM). When indicated, adenine (0.3 mM), guanine (0.3 mM), histidine (0.09 mM), hypoxanthine (0.3 mM), and/or uracil (0.3 mM) were added in SDcasaW medium, resulting in media named SDcasaWA (+ adenine), SDcasaWHypox (+ hypoxanthine), SDcasaWAU (+ adenine + uracil), and SDcasaWU (+ uracil).

Yeast strains and plasmids

All yeast strains are listed in **Table 1** and belong to, or are derived from, a set of disrupted strains isogenic to BY4741 or BY4742 purchased from Euroscarf (Germany). Multi-mutant strains were obtained by crossing, sporulation and micromanipulation of meiosis progeny. The *amd1 aah1 apt1* triple mutant (Y11611) was obtained by disruption of *APT1* in Y2076 using an *APT1*::*URA3* cassette obtained by replacing the 433 bp *Hind*III-*Hind*III fragment of *APT1* (starting 158 bp after ATG) by a *Hind*III-*Hind*III fragment containing *URA* gene. All plasmids are listed in **Table 2**. Cloning details for the unpublished plasmids are available upon request.

Growth test

For drop tests, yeast cells from an overnight pre-culture were re-suspended in sterile water at 1.10^7 cells/ml and submitted to 1/10 serial dilutions. Drops (5 µl) of each dilution were spotted on freshly prepared medium plates and were incubated at 30 or 37 °C for 30–72 h before imaging.

Isolation of mutants and multicopy suppressors of the *amd1 aah1* and *amd1 tat1* adenine-dependent growth defects.

Mutant suppressors of the *amd1 aah1* growth defect in the presence of adenine (Strain Y2076) were selected on SDcasaWUA medium after UV mutagenesis.
Multicopy suppressors of the *amd1 aah1* and *amd1 tat1* adenine-dependent growth defects were obtained by similar procedures. Yeast strains (Y2076 or Y11628) were transformed with a multicopy plasmid library (PFL44L backbone, 2µ *URA3*; generous gift from F. Lacroute). Transformants were selected on SDcasaW medium and gene dosage suppressors were identified by replica-plating of the transformants on SDcasaWA medium and were then verified by drop test on both SDcasaW and SDcasaWA medium. For both multicopy suppressor screens, plasmids from selected clones were extracted and the genomic DNA region inserted in the plasmid was identified by sequencing. When the

identified genomic region contained more than one open reading frame (ORF), each ORF was either subcloned individually or interrupted in the plasmid to unambiguously identify the gene responsible for suppression.

Metabolite extraction and separation by liquid chromatography

Extraction of yeast metabolites was performed by the rapid filtration and ethanol boiling method as described (Loret et al., 2007) and metabolite separation was performed on an ICS3000 chromatography station (Thermofisher) using a carbopac PA1 column (250 x 2 mm; Thermofisher) with the 50 to 800 mM sodium acetate gradient in NaOH 50 mM described in (Ceballos-Picot et al., 2015). Peaks were identified by their retention time as well as co-injection with standards and/or their UV spectrum signature (Ultimate-3000 diode array detector, Thermofisher). Peak area quantifications were done at two different wavelengths: 260 nm for ADP, AMP, ATP, GTP, SAM and SAH and 269 nm for adenine and ZMP. AXP content corresponds to the sum of ATP +ADP + AMP contents. Adenylate energy charge was defined as AEC = (ATP + ½ ADP)/AXP) (Atkinson and Walton, 1967). AXP and AEC were calculated with content of each nucleotide given in nmol/sample (inferred from standard curves using ATP, ADP and AMP pure compounds). For each measurement, presented in figures as mean with standard deviation, metabolic extractions were performed on independent cell cultures and normalization of samples was done on the basis of cell number and median cell volume (determined using a Multisizer 4 (Beckman Coulter)). Statistics were given as p-values determined by a Welch's unpaired t-test.

RESULTS

The severe growth defect of the amd1 aah1 mutant in the presence of adenine is due to GTP shortage

The *amd1* knock-out mutant grown in the presence of adenine showed a mild growth defect (Fig. 2a) accompanied by low GTP and high ATP (Saint-Marc et al., 2009). To enhance the growth phenotype and be able to achieve a suppressor screen, we combined *amd1* with the *aah1* knockout mutation, which further reduces the IMP-supply from adenine (Fig. 1). This genetic combination severely exacerbated the growth defect in the presence of adenine (Saint-Marc et al., 2009), but not in the presence of hypoxanthine that bypasses the lack of *aah1* or in the absence of added purines (Fig.2 a). While metabolic profiling revealed no difference between the two strains in the absence of purines (Supplemental Fig. 1), the *amd1 aah1* mutant upon adenine feeding revealed several major metabolic changes (Fig.2 b-i) that could, either alone or combined, result in the observed growth phenotype. First, we found a severe reduction of intracellular GTP (Fig. 2b) and an increase of ATP (Fig. 2c) similar to what was previously reported for the *amd1* mutation alone (Saint-Marc et al., 2009), although more pronounced for GTP. Of note, in the *amd1 aah1* mutant, the sum of adenylic nucleotides (AXP = ATP + ADP+ AMP) was increased (Fig. 2c-f), showing that the higher intracellular ATP is the result of net adenylic nucleotide synthesis and not merely of enhanced ADP to ATP interconversion. By contrast, adenylic energy charge (AEC = (ATP + ½ ADP)/AXP, Fig. 2g) was the same in the two strains grown in the presence of adenine, thus excluding an energetic defect as responsible for the *amd1 aah1* growth defect (Fig. 2a). In addition, we observed an important accumulation of S-adenosyl-methionine (SAM, Fig. 2h) and S-adenosyl-homocysteine (SAH, Fig. 2i), as previously reported for an *aah1* single mutant (Ceschin et al., 2015). Accumulation of SAH and SAM in the mutant are presumably due to inhibition of SAH hydrolase upon increased intracellular adenine (Fig. 2j)(Knudsen and Yall, 1972) and to inhibition of methyl-transferases by SAH (Zappia et al., 1969), respectively (Fig.1, green dashed lines). We conclude that, in the *amd1 aah1* mutant, in the presence of external adenine, the steady state level

of several metabolites is strongly increased or decreased and we aimed at identifying more precisely which metabolites are responsible for growth impairment through targeted and non-targeted strategies.

While SAM accumulation appears non-toxic for yeast cells (Roje et al., 2002), SAH accumulation was proposed to be toxic in a S-adenosyl-L-homocysteine hydrolase yeast mutant *sah1* (Christopher et al., 2002; Mizunuma et al., 2004; Visram et al., 2018) and could thus contribute to the growth defect of the *amd1 aah1* mutant. The potential role of SAH accumulation in the growth phenotype was assessed by two complementary approaches, the first one was designed to decrease SAH and the second one to increase it. First, we expressed the *E. coli* S-adenosylhomocysteine nucleosidase (*pfs*) enzyme in yeast to lower accumulation of SAM and SAH (Visram et al., 2018). As previously reported, expression of *pfs* suppressed the growth defect of *sah1-1* (Supplemental Fig. 2a) (Visram et al., 2018), but importantly it showed no suppressive effect on the growth defect of the *amd1 aah1* double mutant (Supplemental Fig. 2b). Metabolic profiling confirmed that *pfs* strongly decreased SAH and SAM in the *amd1 aah1* mutant (Supplemental Fig. 2c-d), indicating that high intracellular SAM and SAH in the *amd1 aah1* double mutant are not major causes in the growth defect in the presence of adenine. Of note, *pfs* had no effect on intracellular GTP that remained low (Supplemental Fig. 2e).

Compared to the WT isogenic strain, the *amd1 aah1* mutant accumulated AXP (Fig. 2f) as well as SAM and SAH (Fig. 2h-i). To discriminate these metabolic effects, we combined the *aah1 amd1* mutant with an *apt1* mutant. In this triple mutant adenine cannot be used as a precursor anymore (Fig. 1), but can exert its presumed inhibitory effect on Sah1 (Ceschin et al., 2015; Knudsen and Yall, 1972). We found that the growth defect of the *amd1 aah1* mutant on adenine was fully suppressed by a knockout of *APT1* (Fig. 3a) and that, in the triple *amd1 aah1 apt1* mutant, intracellular ATP was decreased (Fig. 3b) and GTP increased (Fig. 3c). In this mutant, intracellular adenine was increased, as expected due to the incapacity of the *amd1 aah1 apt1* mutant to use this metabolite (Fig. 3d) and, as anticipated, SAM and SAH were even higher than in the *amd1 aah1* double mutant (Fig. 3e-f). Together these results clearly establish that intracellular accumulation of SAM, SAH or adenine is not the cause of the growth defect of the *amd1 aah1* mutant and point to GTP (and possibly ATP) as the critical metabolite for the growth phenotype.

Finally, to address this issue with no *a priori*, we used a non-directed approach based on metabolic profiling of suppressors of the *amd1 aah1* growth defect obtained after UV mutagenesis. Four such suppressors, partially or totally restoring growth of the *amd1 aah1* mutant in the presence of adenine (Supplemental Fig. 3a), were further characterized by metabolic profiling (Supplemental Fig. 3b-f). Clearly, all suppressors increased intracellular GTP (Supplemental Fig. 3b) and decreased ATP (Supplemental Fig. 3c), while SAM, SAH and/or adenine were either increased or decreased depending on the suppressor strain (Supplemental Fig. 3d-f). Thus, this non-directed suppressor strategy nicely confirmed the conclusions drawn from the above metabolite-targeted strategy. Of note, based on their metabolic profiles, we suspected that these suppressor mutations could be allelic to *FCY2* and *APT1* that block adenine uptake and its conversion to AMP (Fig. 1), respectively. These assumptions were validated by sequencing of these loci in the four suppressor strains as well as the corresponding control strain, revealing that the four suppressors correspond to three *fcy2* and one *apt1* mutants (see Table 1). The identity of the suppressors was further confirmed by complementation with the wild-type cognate genes carried on centromeric plasmids (Supplemental Fig. 3g).

Based on these results, the low GTP / high ATP imbalance appeared to be the best candidate to account for *amd1 aah1* growth defect. Accordingly, guanine supplementation improved growth of the mutant in the presence of adenine although not restoring wild-type growth (Fig. 4a). However, when the same strains were grown in liquid medium for metabolic profiling experiments, we observed a complete

restoration of growth in the presence of adenine and guanine (Fig. 4b). This discrepancy could be due to the very poor solubility of guanine that could limit its diffusion on plates. Metabolic profiling in the presence of guanine confirmed a restoration, though partial, of intracellular GTP and ATP (Fig. 4c-d). From these results, we conclude that low intracellular GTP (possibly in combination with high ATP) is responsible for the growth defect of *amd1 aah1* mutant in the presence of adenine, while no significant role for accumulation of SAM or SAH could be established.

Gene dosage suppressors refuel the GTP synthesis through de novo pathways

To get further understanding on the causes of the *amd1 aah1* growth defect, we searched for gene-dosage suppressors that would restore growth of the *amd1 aah1* mutant in the presence of adenine. A yeast genomic multicopy plasmid library was transformed in the *amd1 aah1* mutant and 52 transformants, showing improved capacity to grow in the presence of adenine, were studied. Among those, 20 plasmids contained either *AAH1* or *AMD1*, hence complementing one of the two mutations of the double mutant, and were not further studied. The remaining plasmids were extracted and retransformed in the *amd1 aah1* mutant and we could identify 15 plasmids that were clearly sufficient to restore growth of the *amd1 aah1* mutant in the presence of adenine. Eight plasmids contained a region of chromosome II carrying the *TAT1* gene as the only common entire coding region. Four plasmids contained a region carrying the *ADE4* gene and one carried the *HIS1* gene. One plasmid contained the *PIK1* gene alone and the last plasmid carried a region of chromosome IV containing three entire open reading frames (*RPL35B*, *RDI1* and *PPH21*). Further experiments confirmed *TAT1*, *ADE4*, *HIS1*, *PIK1* and *PPH21* as the dosage suppressor genes (Fig. 5a-b). *TAT1* encodes an amino acid transporter, *ADE4* and *HIS1* encode the first enzymes of purine and histidine *de novo* pathways respectively, *PIK1* encodes a phosphatidylinositol 4-kinase and *PPH21 (*with *PPH22)* encodes the catalytic subunit of protein phosphatase 2A, PP2A. *TAT1*, *HIS1* and *ADE4* were the strongest suppressors while *PIK1* and *PPH21* were both weak suppressors (Fig. 5a-b). Of note, *PIK1* suppression was more efficient at 30°C (Fig. 5a), while *PPH21* suppressed better at 37°C (Fig. 5b).

The effect of each gene dosage suppressor on intracellular GTP was evaluated (Fig. 5c). *ADE4* and *HIS1* overexpression partially replenished intracellular GTP thus explaining their suppression effect most probably through fueling of IMP synthesis *via* the purine or histidine *de novo* pathway, respectively (Fig. 1). Indeed, both Ade4 and His1 have been shown previously to be controlling enzymes, tightly feedback inhibited by the end-products of the cognate pathways, ATP and histidine, respectively (Rasse-Messenguy and Fink, 1973; Rebora et al., 2001). The dual contribution of histidine and purine synthesis to the *amd1 aah1* growth phenotype was further established by the fact that concomitant repression of the two pathways by adenine and histidine was required to observe the *amd1 aah1* growth phenotype (Fig. 5d) as well as the intracellular GTP decrease (Fig. 5e). We conclude that GTP refueling *via* enhanced flux through the histidine or purine *de novo* pathway is sufficient to restore growth of the *amd1 aah1* mutant in good agreement with our previous observation of phenotypic suppression by exogenous guanine (Fig. 4). Of note, the gene dosage suppressors had no significant effect on intracellular ATP (Fig. 5f), indicating that intracellular GTP or the purine nucleotide balance is the critical factor responsible for the slow growth phenotype.

The suppressor effect of TAT1, PIK1 and PPH21 overexpression requires a functional histidine pathway

TAT1, the strongest suppressor, had a mild, though highly significant, effect on GTP (Fig. 5c) suggesting that it could, at least in part, act *via* one or both the GTP refueling routes, namely *de novo* purine or histidine pathways. Clearly, *TAT1* overexpression had no suppressive effect in the *aah1 amd1*

ade8 his1 strain blocking both the histidine and the purine *de novo* pathway (Fig. 6a). To discriminate between these two routes, *TAT1* was overexpressed in *amd1 ade4* and *amd1 his1* double mutants. In the *amd1 ade4* strain, *TAT1* was an efficient suppressor, while the suppression was totally abolished in the *amd1 his1* mutant (Fig. 6b). We conclude that suppression by *TAT1* overexpression requires a functional histidine biosynthesis pathway. This result suggests that *TAT1* overexpression (just as that of *HIS1*) acts by increasing the flux in the histidine pathway resulting in increased synthesis of ZMP (which is a by-product of histidine synthesis, Fig. 1) and a precursor of IMP and GMP synthesis (Fig. 1). Accordingly, in an *ade16 ade17* mutant background, blocking ZMP consumption and allowing to monitor its accumulation, we found that overexpression of *TAT1* increased ZMP in an *ade16 ade17*, as well as in an *ade16 ade17 ade8* but not in an *ade16 ade17 his1* mutants (Fig. 6c). From all these experiments, we conclude that *TAT1* acts as a suppressor by increasing the histidine pathway flux and thereby fueling the purine pathway *via* ZMP (Fig. 1). It is noteworthy that suppression due to *TAT1* overexpression was not dependent on the presence of the transcription factor Gcn4 that activates the histidine biosynthesis genes (Ljungdahl and Daignan-Fornier, 2012). Indeed, suppression by *TAT1* was similarly effective in the *amd1* and the *amd1 gcn4* mutants (Supplemental Fig. 4). Finally, as for *TAT1*, we found that suppression by overexpression of *PIK1* and *PPH21* required a functional histidine biosynthesis pathway (Fig. 6d). Hence, our results show that the three gene dosage suppressors *TAT1*, *PIK1* and *PPH21* act through the histidine pathway and suggest that they could participate to a common mechanism.

The amd1 tat1 double mutant shows a strong synthetic phenotype: identification of suppressors

The results presented in the previous section established that *TAT1* overexpression interferes with purine nucleotide synthesis, and significantly on GTP, through the enhancement of the histidine pathway. Strikingly, our previous work had revealed that a *tat1* knockout mutation resulted in increased sensitivity to GTP shortage associated to treatment of yeast with mycophenolic acid (MPA) an immunosuppressive drug that operates by inhibiting IMP dehydrogenase (IMPDH) (Desmoucelles et al., 2002). Henceforth, overexpression of *TAT1* can suppress the GTP-shortage associated growth defect of the *amd1* and *amd1 aah1* mutants, while the lack of *tat1* rendered yeast cells more sensitive to GTP shortage. To examine further the relationship between Tat1 and GTP, we combined *tat1* and *amd1* mutations. As anticipated from increased MPA-sensitivity (Desmoucelles et al., 2002), the double mutant showed a synthetic growth defect specifically in the presence of adenine (Fig. 7a), when intracellular GTP is low in the *amd1* mutant. However, strikingly, this enhancement of the *amd1* phenotype by *tat1* was not associated to a further decrease of intracellular GTP, by contrast to what was observed for the *amd1 aah1* mutant combination (Fig. 7b). Hence, *TAT1* overexpression suppressed the growth defect of the *amd1 aah1* mutant by increasing intracellular GTP (Fig. 5c), while *tat1* mutation enhanced the *amd1* phenotype without further altering intracellular GTP (Fig. 7b). We conclude that *TAT1* over- and under-expression act through different means.

To examine further the synthetic growth phenotype of the *amd1 tat1* mutant, we isolated gene dosage suppressors that alleviate the growth defect of the double mutant in the presence of adenine. A set of 95 plasmids suppressing the growth defect of the *amd1 tat1* mutant were analyzed. Among those, 45 carried the *TAT1* gene and 22 the *AMD1* gene, hence confirming that the phenotype is the result of the combination of the two mutations. The *bona fide* gene dosage suppressors include several genes involved in purine metabolism (*ADE4*, *AAH1*, *APT2*, *HPT1*, *XPT1*), but also the *PPH21* gene previously isolated in the *amd1 aah1* screen (see prior sections) and four new genes (*ERC1*, *HYM1*, *MSN2* and *BAP2*) exhibiting various suppression strength (Supplemental Fig. 5). Metabolic profiling of the suppressors (Fig. 7c) showed that most of them, excepting MSN2, *BAP2* and *HYM1*, significantly

increased intracellular GTP, suggesting that they act through replenishing IMP and GMP biosynthesis *via* the *de novo* pathway (*ADE4*) or the salvage pathway (*AAH1*, *HPT1*). *XPT1* was initially described as a gene dosage suppressor of *HPT1* (Guetsova et al., 1999) and could hence phenocopy *HPT1* overexpression for suppression of *amd1 tat1*. Two suppressors (*ERC1* and *HYM1*) increased intracellular SAH and SAM (Fig. 7d-e). In the case of *ERC1* this effect was very strong as previously reported (Kanai et al., 2017). *ERC1* encodes a member of the multi-drug and toxin extrusion family. It is not clear why its overexpression should suppress the *amd1 tat1* growth defect. However, the fact that the suppression by *ERC1* is associated to higher intracellular GTP, as well as higher SAM and SAH (Fig. 7c-e), confirmed that accumulation of the latter two metabolites is not involved in the mutant growth phenotype.

The identification of *APT2* as a gene dosage suppressor of *amd1 tat1* was quite surprising since Apt2 is presumed to have no APRT activity (Alfonzo et al., 1999) and that, in any case, overexpression of APRT rather exacerbated than improved the growth phenotype of the *amd1* mutant (Saint-Marc et al., 2009). Indeed, overexpression of the two paralogues, *APT1* and *APT2*, had opposite effects on the growth of *amd1* in the presence of adenine, while *APT2* overexpression clearly suppressed *amd1*; *APT1* enhanced its growth defect (Fig. 7f). Whether suppression by *APT2* was dependent on Apt1 was tested in an *amd1 apt1 tat1* triple mutant (Supplemental Fig. 6) but no conclusion could be drawn since *amd1 tat1* was robustly suppressed by *apt1*, similarly to what we found previously for *aah1 amd1* (Fig. 3A) Thus, we conclude that *APT2* rather counteracts than mimics *APT1* phenotypically. Of note, in the BY background, *apt2* was neither synthetic lethal with *apt1* (Supplemental Fig. 7) nor *aah1* (Supplemental Fig. 8), by contrast to what was reported in SGD database based on a genome-wide analysis (Deutscher et al., 2006).

DISCUSSION

Deciphering the precise metabolic defect responsible for the growth phenotype

This work illustrates how simple metabolic blocks can result in conditional accumulation or defect of multiple metabolites. This complex profile is due to the untangled architecture of the metabolic network, which favors robustness but makes phenotypic interpretation difficult. Yeast genetics clearly allowed addressing separately the contribution of these metabolites to the growth phenotype. Interestingly, a metabolite such as SAH, supposedly highly toxic, accumulated under conditions of robust growth (for example *amd1 aah1 apt1* mutant Fig. 3) suggesting that combinations of faulty metabolites, rather than a single defect, are contributing to the phenotypic outcome making it difficult to understand completely. This work exemplifies, in a very simple isogenic situation, the complex interplay between pleiotropy (several metabolites affected and most probably several downstream functions impaired) and external conditions (presence of various purine precursors at constantly varying concentrations in the cellular environment, variable suppression efficiency depending on temperature, liquid versus solid medium…). It therefore strongly questions our future capability to predict accurately phenotype from genotype.

Suppression patterns suggest pleiotropy

Strikingly, all the suppressors of the *amd1 aah1* growth defect in the presence of adenine restored at least partially GTP and the ATP/GTP balance, hence confirming that it is most likely causative of the growth phenotype. The fact that no suppressors were found restoring functionally downstream processes that could be affected by low GTP or purine imbalance, strongly suggests that there is not a single limiting factor but, instead, that the metabolic defect is most probably pleiotropic. A serious candidate-

function is protein translation that was found altered in a yeast *gua1* mutant limiting GMP synthesis from IMP (Iglesias-Gato et al., 2011) and also in *amd1* and human *AMPD2* defective cells (Akizu et al., 2013). However, GTP is required at many steps in the translation process and our suppressor screen did not point to any single critical step. Our results rather suggest that replenishment of the GTP pool and/or GTP/ATP balance should be the target of future treatments.

TAT1 is tightly connected to intracellular GTP

TAT1 was identified as a robust gene dosage suppressor and its suppression ability was clearly dependent on the histidine synthesis pathway. The precise mechanism is unknown but *TAT1* overexpression strongly stimulated ZMP synthesis when the histidine pathway was the only possible route (in the *ade8 ade16 ade17* mutant Fig. 6c). This connection, between an amino acid transporter, which is not a major histidine carrier, and the histidine biosynthesis pathway is intriguing. We found that suppression due to *TAT1* overexpression was not dependent on the presence of Gcn4 which is a major transcription factor involved in expression of the histidine biosynthesis genes (Ljungdahl and Daignan-Fornier, 2012). The mechanism connecting *TAT1* to the histidine pathway remains to be clarified but is complicated by the fact that *tat1* knock-out interferes with *amd1* through a different mean. Indeed, our previous work revealed an exacerbated sensitivity of the *tat1* knock-out mutant to mycophenolic acid, a specific inhibitor of GTP synthesis (Desmoucelles et al., 2002). Here we found that the *amd1* mutant was synthetic sick with *tat1* specifically in the presence of adenine leading to low intracellular GTP. However, by contrast to synthetic sickness of *amd1* with *aah1*, *tat1* did not exacerbate the intracellular GTP defect. Gene dosage suppressors revealed that there are two ways to suppress this growth defect. Either by replenishing the GTP pool by overexpression of purine interconversion genes, or by overexpressing the amino acid transporter Bap2 (Fig. 7). Together our data point to a strong phenotypic connection between amino acid uptake and GTP synthesis.

Interestingly, *PIK1* another gene dosage suppressor identified in this work also requires a fully functional histidine pathway to suppress the *aah1 amd1* growth phenotype. The link between this inositol kinase and GTP synthesis is potentially highly relevant since another inositol kinase was shown to sense GTP and respond to it (Sumita et al., 2016). Identifying further connections between guanine nucleotides and inositol derivatives could prove to be physiologically very important considering the key roles played by these metabolites.

What function for APT2?

Suppression of the *amd1 tat1* mutant revealed gene dosage suppressors that increase intracellular GTP and others, such as *BAP2*, that probably partially compensate for the *tat1* defect. Among suppressors partially restoring intracellular GTP, most can be interpreted as redirecting adenine to IMP via hypoxanthine (*AAH1*, *HPT1*, *XPT1*) or *via* the purine *de novo* pathway (*ADE4*) (Fig. 1). Among these suppressor genes, identification of *APT2* was surprising. *APT2* does not code for functional APRT (Alfonzo et al., 1999) and in any case, *APT1* overexpression enhances the *amd1* phenotype while *APT2* was a gene dosage suppressor (Fig. 7f). Our results hence rather indicate that *APT2* antagonizes *APT1* as was previously proposed (Carlsson et al., 2018). This situation is remindful of what we reported for Ybr284w and Yjl070c, two paralogs of Amd1, that, when overexpressed, were shown to mimic *amd1* knockout (Saint-Marc et al., 2009). Hence, the fact that paralogs can antagonize each other could be a recurrent feature of metabolism in yeast.

Concluding remark

In a more general perspective, understanding the effects of GTP deprivation and ATP/GTP imbalance could be of great value to understand how purine biosynthesis and interconversion affect complex diseases such as for example cancer. Indeed nucleotides are central in cancer cell metabolism but their dual roles as energy suppliers and building blocks are difficult to separate (Vander Heiden and DeBerardinis, 2017). In yeast, the effects of GTP deprivation and ATP/GTP imbalance on gene expression have been explored and proved complex (Hesketh et al., 2019; Saint-Marc et al., 2009). The high pleiotropy, due to the central role of these metabolites in multiple key processes within the cell, makes it difficult to address experimentally, but yeast has proved to be a good model to tackle this problem (Hesketh and Oliver, 2019).

References

Akizu, N., Cantagrel, V., Schroth, J., Cai, N., Vaux, K., McCloskey, D., Naviaux, R.K., Van Vleet, J., Fenstermaker, A.G., Silhavy, J.L*., et al.* (2013). AMPD2 regulates GTP synthesis and is mutated in a potentially treatable neurodegenerative brainstem disorder. Cell *154*, 505-517.

Alfonzo, J.D., Crother, T.R., Guetsova, M.L., Daignan-Fornier, B., and Taylor, M.W. (1999). APT1, but not APT2, codes for a functional adenine phosphoribosyltransferase in Saccharomyces cerevisiae. J Bacteriol *181*, 347-352.

Atkinson, D.E., and Walton, G.M. (1967). Adenosine triphosphate conservation in metabolic regulation. Rat liver citrate cleavage enzyme. J Biol Chem *242*, 3239-3241.

Bonneaud, N., Ozier-Kalogeropoulos, O., Li, G.Y., Labouesse, M., Minvielle-Sebastia, L., and Lacroute, F. (1991). A family of low and high copy replicative, integrative and single-stranded S. cerevisiae/E. coli shuttle vectors. Yeast *7*, 609-615.

Carlsson, M., Hu, G.Z., and Ronne, H. (2018). Gene dosage effects in yeast support broader roles for the LOG1, HAM1 and DUT1 genes in detoxification of nucleotide analogues. PLoS One *13*, e0196840.

Ceballos-Picot, I., Le Dantec, A., Brassier, A., Jais, J.P., Ledroit, M., Cahu, J., Ea, H.K., Daignan-Fornier, B., and Pinson, B. (2015). New biomarkers for early diagnosis of Lesch-Nyhan disease revealed by metabolic analysis on a large cohort of patients. Orphanet J Rare Dis *10*, 7.

Ceschin, J., Hurlimann, H.C., Saint-Marc, C., Albrecht, D., Violo, T., Moenner, M., Daignan-Fornier, B., and Pinson, B. (2015). Disruption of Nucleotide Homeostasis by the Antiproliferative Drug 5-Aminoimidazole-4-carboxamide-1-beta-d-ribofuranoside Monophosphate (AICAR). J Biol Chem *290*, 23947-23959.

Christopher, S.A., Melnyk, S., James, S.J., and Kruger, W.D. (2002). S-adenosylhomocysteine, but not homocysteine, is toxic to yeast lacking cystathionine beta-synthase. Mol Genet Metab *75*, 335-343.

Daignan-Fornier, B., and Pinson, B. (2019). Yeast to Study Human Purine Metabolism Diseases. Cells *8*.

Desmoucelles, C., Pinson, B., Saint-Marc, C., and Daignan-Fornier, B. (2002). Screening the yeast "disruptome" for mutants affecting resistance to the immunosuppressive drug, mycophenolic acid. J Biol Chem *277*, 27036-27044.

Deutscher, D., Meilijson, I., Kupiec, M., and Ruppin, E. (2006). Multiple knockout analysis of genetic robustness in the yeast metabolic network. Nat Genet *38*, 993-998.

Gari, E., Piedrafita, L., Aldea, M., and Herrero, E. (1997). A set of vectors with a tetracycline-regulatable promoter system for modulated gene expression in Saccharomyces cerevisiae. Yeast *13*, 837-848.

Gietz, R.D., and Sugino, A. (1988). New yeast-Escherichia coli shuttle vectors constructed with in vitro mutagenized yeast genes lacking six-base pair restriction sites. Gene *74*, 527-534.

Guetsova, M.L., Crother, T.R., Taylor, M.W., and Daignan-Fornier, B. (1999). Isolation and characterization of the Saccharomyces cerevisiae XPT1 gene encoding xanthine phosphoribosyl transferase. J Bacteriol *181*, 2984-2986.

Hesketh, A., and Oliver, S.G. (2019). High-energy guanine nucleotides as a signal capable of linking growth to cellular energy status via the control of gene transcription. Curr Genet *65*, 893-897.

Hesketh, A., Vergnano, M., and Oliver, S.G. (2019). Determination of the Global Pattern of Gene Expression in Yeast Cells by Intracellular Levels of Guanine Nucleotides. mBio *10*.

Iglesias-Gato, D., Martin-Marcos, P., Santos, M.A., Hinnebusch, A.G., and Tamame, M. (2011). Guanine nucleotide pool imbalance impairs multiple steps of protein synthesis and disrupts GCN4 translational control in Saccharomyces cerevisiae. Genetics *187*, 105-122.

Kanai, M., Kawata, T., Yoshida, Y., Kita, Y., Ogawa, T., Mizunuma, M., Watanabe, D., Shimoi, H., Mizuno, A., Yamada, O*., et al.* (2017). Sake yeast YHR032W/ERC1 haplotype contributes to high S-adenosylmethionine accumulation in sake yeast strains. J Biosci Bioeng *123*, 8-14.

Knudsen, R.C., and Yall, I. (1972). Partial purification and characterization of S-adenosylhomocysteine hydrolase isolated from Saccharomyces cerevisiae. J Bacteriol *112*, 569-575.

Ljungdahl, P.O., and Daignan-Fornier, B. (2012). Regulation of amino acid, nucleotide, and phosphate metabolism in Saccharomyces cerevisiae. Genetics *190*, 885-929.

Loret, M.O., Pedersen, L., and Francois, J. (2007). Revised procedures for yeast metabolites extraction: application to a glucose pulse to carbon-limited yeast cultures, which reveals a transient activation of the purine salvage pathway. Yeast *24*, 47-60.

Mizunuma, M., Miyamura, K., Hirata, D., Yokoyama, H., and Miyakawa, T. (2004). Involvement of S-adenosylmethionine in G1 cell-cycle regulation in Saccharomyces cerevisiae. Proc Natl Acad Sci U S A *101*, 6086-6091.

Pinson, B., Vaur, S., Sagot, I., Coulpier, F., Lemoine, S., and Daignan-Fornier, B. (2009). Metabolic intermediates selectively stimulate transcription factor interaction and modulate phosphate and purine pathways. Genes Dev *23*, 1399-1407.

Rasse-Messenguy, F., and Fink, G.R. (1973). Feedback-resistant mutants of histidine biosynthesis in yeast. Basic Life Sci *2*, 85-95.

Rebora, K., Desmoucelles, C., Borne, F., Pinson, B., and Daignan-Fornier, B. (2001). Yeast AMP pathway genes respond to adenine through regulated synthesis of a metabolic intermediate. Mol Cell Biol *21*, 7901-7912.

Rebora, K., Laloo, B., and Daignan-Fornier, B. (2005). Revisiting purine-histidine cross-pathway regulation in Saccharomyces cerevisiae: a central role for a small molecule. Genetics *170*, 61-70.

Roje, S., Chan, S.Y., Kaplan, F., Raymond, R.K., Horne, D.W., Appling, D.R., and Hanson, A.D. (2002). Metabolic engineering in yeast demonstrates that S-adenosylmethionine controls flux through the methylenetetrahydrofolate reductase reaction in vivo. J Biol Chem *277*, 4056-4061.

Saint-Marc, C., Pinson, B., Coulpier, F., Jourdren, L., Lisova, O., and Daignan-Fornier, B. (2009). Phenotypic consequences of purine nucleotide imbalance in Saccharomyces cerevisiae. Genetics *183*, 529-538, 521SI-527SI.

Sumita, K., Lo, Y.H., Takeuchi, K., Senda, M., Kofuji, S., Ikeda, Y., Terakawa, J., Sasaki, M., Yoshino, H., Majd, N*., et al.* (2016). The Lipid Kinase PI5P4Kbeta Is an Intracellular GTP Sensor for Metabolism and Tumorigenesis. Mol Cell *61*, 187-198.

Vander Heiden, M.G., and DeBerardinis, R.J. (2017). Understanding the Intersections between Metabolism and Cancer Biology. Cell *168*, 657-669.

Visram, M., Radulovic, M., Steiner, S., Malanovic, N., Eichmann, T.O., Wolinski, H., Rechberger, G.N., and Tehlivets, O. (2018). Homocysteine regulates fatty acid and lipid metabolism in yeast. J Biol Chem *293*, 5544-5555.

Zappia, V., Zydek-Cwick, R., and Schlenk, F. (1969). The specificity of S-adenosylmethionine derivatives in methyl transfer reactions. J Biol Chem *244*, 4499-4509.

Figure legends

Fig. 1 Schematic representation of the *de novo* purine and histidine pathways and of the methyl cycle in yeast. Only the enzymes mentioned in the text are shown (in red). *AMP* adenosine 5'-monophosphate, *GMP* Guanosine 5′-monophosphate, *IMP* Inosine 5′-monophosphate, *PRFZMP* N-5-phosphoribosyl-formimino-5-amino-imidazole-4-carboxamide ribonucleotide monophosphate, *PRPP* α-D-ribofuranose 5-phosphate 1-diphosphate, *SAH* S-adenosyl-L-homocysteine, *SAM* S-adenosyl-L-methionine, *XMP* xanthosine 5′-monophosphate and *ZMP* 5-amino-imidazole 4-carboxamide ribonucleotide 5'-monophosphate (also known as AICAR monophosphate). The dashed green lines show the inhibition of the S-adenosyl homocysteine hydrolase activity by adenine and of the methyl-transferases by S-adenosyl-L-homocysteine (see text).

Fig. 2 Growth alteration of the *amd1 aah1* double mutant in the presence of adenine is associated with changes in the steady state level of several purine derivatives. **a** Adenine supplementation strongly affects proliferation of an *amd1 aah1* double mutant. Yeast cells (Y175, Y2076, Y4198 and Y6750) were serial diluted and grown for 48 hours at 30°C on SDcasaWU medium supplemented or not with indicated purines. **b-j** Metabolic changes associated to adenine supplementation in the *amd1 aah1* double mutant. Y175 (wild-type (WT), blue dots) and Y2076 (red dots) were exponentially grown for 24 h in SDcasaWU and adenine was added for 4 h before metabolic extraction. Metabolites were then separated by liquid chromatography, quantifications were determined on biologically independent extractions and standard deviation is presented. For each metabolite, the amount measured in wild-type cells (blue dots) was set at 1. Numbers on the top of each panel correspond to the p-value calculated from a Welch's unpaired t-test. **h-j** the dashed blue line illustrates scale breaks. **a-j** Of note, media used in this figure contains 0.3 mM of histidine from the casamino-acids mixture.

Fig. 3 Deletion of *APT1* is sufficient to restore both proliferation and intracellular purine nucleotide triphosphate level in the *amd1 aah1* mutant. **a** The adenine-dependent growth defect of the *amd1 aah1* mutant was fully suppressed by *APT1* knockout. Dilutions of BY4742 (wild-type), Y2076 and Y11611 strains were spotted on SDcasaWU medium (containing 0.3 mM of histidine) supplemented or not with adenine and grown for 40 h at 30°C. **b-f** Restoration of ATP and GTP levels by deletion of *APT1*. Strains (Y2076 and Y11611) were grown in SDcasaWU medium and adenine was added for 4 h before metabolic extraction, separation and quantification done as in Fig. 2. For each metabolite, the amount measured in the *amd1 aah1* cells was set at 1 (red dots). Numbers on the top of each panel correspond to the p-value calculated from a Welch's unpaired t-test.

Fig. 4 Alteration of *amd1 aah1* proliferation by adenine is alleviated by guanine supplementation and is associated to a partial restoration of the GTP/ATP imbalance. **a-b** Guanine supplementation suppresses either partially on plates (**a**) or totally in liquid (**b**) the proliferation defect of the *amd1 aah1* mutant. **a** BY4741 (wild-type) and Y2076 strains were serial diluted and grown for 30 hours at 30°C on SDcasaWU medium supplemented or not with indicated purines. **b** The *amd1 aah1* mutant (Y2076) was exponentially grown for 24 hours in SDcasaWU and diluted to $2x10^6$ cells/ml in the same medium containing or not adenine (green and blue dots) and guanine (blue dots). Cell proliferation was followed using a Multisizer IV (Beckman Coulter). **c-d** ATP (**c**) and GTP (**d**) relative contents are partially restored under guanine supplementation. Metabolic extraction, separation and quantification were done as in Fig. 2 on the *amd1 aah1* mutant shifted (Y2076) for 4 h to SDcasaWU medium supplemented or not (red dots) with adenine (green dots) or adenine + guanine (blue dots). For each metabolite, the

amount measured in cells grown in the absence of purine (red dots) was set at 1. Numbers correspond to the p-value calculated from a Welch's unpaired t-test.

Fig. 5 Gene dosage suppressors alleviate the adenine-dependent growth defect of the *amd1 aah1* mutant in a GTP-refueling dependent manner. **a-c, f** Wild-type (WT, Y175) and *amd1 aah1* (Y2076) strains were transformed with plasmids allowing overexpression (OE) or not (None) of indicated genes (p5839, p5840, p5841, p5842 and p5847 for *TAT1*, *PIK1*, *ADE4*, *HIS1* and *PPH21*, respectively). **a-b** Transformants were serial diluted and grown for 48 h on SDcasaW medium (containing 0.3 mM of histidine (His) from casamino-acids) supplemented or not with adenine (Ade) at 30 °C (**a**) and 37°C (**b**). **c** GTP relative level is increased in most of the gene dosage suppressors. Transformants were exponentially grown for 24 h in SDcasaW medium and then adenine was added for 4 h before metabolite extraction. The amount of GTP measured in wild-type cells transformed by the control plasmid (None, blue dots) was set at 1. **d-e** Histidine and purine pathways are both required to observe a growth defect and a GTP drop in the *amd1 aah1* mutant. **d** Y2076 strain was transformed with the *HIS3 LEU2* centromeric plasmid (p2191, which renders it prototrophic for histidine) and with plasmids allowing overexpression of either *HIS1* (p3332) or *ADE4* (p1933) genes or by the cognate control vectors (None, pCM189 or PFL44L). Serial dilutions were spotted on SD medium ± Adenine (0.3 mM) ± Histidine (0.09 mM) and plates were imaged after 48 h at 30°C. **e** The *amd1 aah1* mutant (Y2076) containing the *HIS3 LEU2* plasmid was exponentially grown for 24 h in SDU medium and then GTP levels were determined after a 4 h incubation in the presence or absence of adenine and/or histidine. The amount of GTP measured in cells grown in the absence of supplement (No addition) was set at 1. **f** ATP relative content determined in the metabolic extracts from Fig. 5c. **c**, **e-f** Numbers correspond to the p-value calculated from a Welch's unpaired t-test.

Fig. 6 A functional histidine pathway is required for the gene dosage suppression of the *amd1* proliferation phenotype. **a-b** Suppression of the *amd1 aah1* growth phenotype by *TAT1* overexpression is inoperative in the absence of histidine pathway. Yeast strains (Y2690, Y11779, Y11784 and Y11821) were transformed with a plasmid allowing *TAT1* overexpression (OE, p5839) or by the empty vector (None, pFL44L). Transformants were grown for 48 h at 30 °C on SDcasaW medium containing 0.3 mM of histidine (from casamino-acids) and the indicated source of purine. **c** *TAT1* overexpression results in an increased level of ZMP synthetized from the histidine pathway. Yeast (Y1162, Y2787 and Y4423) were transformed with the *TAT1* overexpression plasmid or the cognate empty vector (None). ZMP level were determined on cells grown in SDcasaWA medium as described in Fig. 2. The amount measured in *ade16 ade17* cells with the empty vector (light orange dots) was set at 1. Numbers correspond to the p-value calculated from a Welch's unpaired t-test. **d** A functional histidine pathway is required for suppressor effect of *PPH21* and *PIK1* on *amd1* mutant proliferation. Y11643, Y11782 and Y11821 yeast strains were transformed with an empty vector (None, PFL44L) or with plasmids overexpressing (OE) the indicated genes (p5839, p5840 and p5847). Transformants were grown for 48 h at 30°C on SDcasaW medium containing the indicated source of purine.

Fig. 7 Suppressors effect on the proliferation and metabolic phenotypes associated with the *amd1 tat1* mutant. **a-b** The *amd1 tat1* double mutant displays a severe growth defect but not associated to an enhanced GTP decrease compared to *amd1*. Yeast strains (BY4742 (wild-type), Y1031, Y2076 and Y11627) were serial diluted and grown for 48 h at 30°C on SDcasaWU medium (containing 0.3 mM of histidine from casamino-acids) supplemented or not with adenine (**a**) or were exponentially grown in SDcasaWU medium for 24 h and adenine was added 4 h before being submitted to a metabolic extraction and GTP quantification as in Fig. 2 (**b**). GTP level determined in wild type cells (blue dots) was set at 1. **c-e** Metabolic profiling of the *amd1 tat1* gene-dosage suppressors. The *amd1 tat1* double mutant strain

was transformed with plasmids overexpressing (OE) the indicated genes (p5894, p5896, p5897, p5898, p5899, p5900, p5901, p5902 and p6026 for *XPT1*, *ADE4*, *HYM1*, *ERC1*, *MSN2*, *BAP2*, *AAH1*, *HPT1* and *APT2* or by the empty vector (None, pFL44L). Transformants were exponentially grown for 24 h in SDcasaWU medium, adenine was then added for 4 h prior to metabolic extraction as in Fig. 2. For each metabolite, the level determined in cells containing the empty vector (orange dots) was set at 1. **b-e** Numbers correspond to the p-value calculated from a Welch's unpaired t-test. **f** Growth of *amd1* in the presence of adenine is restored by overexpression of *APT2* but not *APT1*. The *amd1* mutant (Y11784) was transformed by plasmids allowing overexpression of *APT1* (p5011) or *APT2* (p552) or by the empty vector (None, YepLac195). Transformants were serial diluted and growth was imaged after 48 h at 30°C on SDcasaW medium ± adenine.

Table 1 Yeast strains used in this study

Strain	Genotype	References
BY4741	*MAT***a** *his3Δ1 leu2Δ0 ura3Δ0 met15Δ0*	Euroscarf
BY4742	*MATα his3Δ1 leu2Δ0 ura3Δ0 lys2Δ0*	Euroscarf
Y175	*MAT***a** *his3Δ1 leu2Δ0 ura3Δ0*	This study
Y1031	*MAT***a** *his3Δ1 leu2Δ0 ura3Δ0 met15Δ0 amd1::KanMX4*	Euroscarf
Y1162	*MATα his3Δ1 leu2Δ0 ura3Δ0 ade16::KanMX4 ade17::KanMX4*	(Pinson et al., 2009)
Y2076	*MAT***a** *his3Δ1 leu2Δ0 ura3Δ0 aah1::KanMX4 amd1::KanMX4*	This study
Y2690	*MATα his3Δ1 leu2Δ0 lys2Δ0 ura3Δ0 aah1::KanMX4 amd1::KanMX4 ade8::KanMX4 his1::KanMX4*	This study
Y2787	*MAT***a** *his3Δ1 leu2Δ0 ura3Δ0 met15Δ0 his1::KanMX4 ade16::KanMX4 ade17::KanMX4*	(Pinson et al., 2009)
Y4198	*MAT***a** *his3Δ1 leu2Δ0 ura3Δ0 amd1::KanMX4*	This study
Y4423	*MAT***a** *his3Δ1 leu2Δ0 ura3Δ0 ade8::KanMX4 ade16::KanMX4 ade17::KanMX4*	This study
Y5941	*MAT***a** *trp1 leu2 ade2 ura3 his3 can1-100 sah1-1*	(Mizunuma et al., 2004)
Y6750	*MAT***a** *his3Δ1 leu2Δ0 ura3Δ0 aah1::KanMX4*	(Ceschin et al., 2015)
Y11611	*MAT***a** *his3Δ1 leu2Δ0 ura3Δ0 aah1::KanMX4 amd1::KanMX4 apt1::URA3*	This study
Y11627	*MAT***a** *his3Δ1 leu2Δ0 ura3Δ0 lys2Δ0 met15Δ0 tat1::KanMX4 amd1::KanMX4*	This study
Y11643	*MAT***a** *his3Δ1 ura3Δ0 amd1::KanMX4*	This study
Y11779	*MAT***a** *ura3Δ0 ade4::KanMX4 amd1::KanMX4*	This study
Y11782	*MAT***a** *ura3Δ0 leu2Δ0 ade4::KanMX4 amd1::KanMX4*	This study
Y11784	*MAT***a** *ura3Δ0 amd1::KanMX4*	This study
Y11821	*MATα his3Δ1 leu2Δ0 ura3Δ0 his1::KanMX4 amd1::KanMX4*	This study

Table 2 Plasmids used in this study

Plasmid	Backbone	Characteristics	References
pCM189	pCM189	*CEN ARS URA3 tet-OFF promoter*	(Gari et al., 1997)
YCpLac111	YCpLac111	*CEN ARS LEU2*	(Gietz and Sugino, 1988)
YEpLac195	YEpLac195	2 μm *URA3*	(Gietz and Sugino, 1988)
pFL44L	pFL44L	2 μm *URA3*	(Bonneaud et al., 1991)
p1933	pCM189	*CEN ARS URA3 tet-OFF prom-ADE4*	(Rebora et al., 2001)
p2191	YCpLac111	*CEN ARS LEU2 HIS3*	(Rebora et al., 2005)
P3332	pFL44L	2 μm *URA3 HIS1*	Lab Collection
p5011	YEpLac195	2 μm *URA3 APT1*	Lab Collection
p5839	pFL44L	2 μm *URA3 TAT1*	This study
p5840	pFL44L	2 μm *URA3 PIK1*	This study
p5841	pFL44L	2 μm *URA3 ADE4*	This study
p5842	pFL44L	2 μm *URA3 HIS1*	This study
p5847	pFL44L	2 μm *URA3 RPL35B-RDI1-PPH21*	This study
p5894	pFL44L	2 μm *URA3 XPT1*	This study
p5896	pFL44L	2 μm *URA3 ADE4 LIP1 DIN3*	This study
p5897	pFL44L	2 μm *URA3 HYM1*	This study
p5898	pFL44L	2 μm *URA3 ERC1*	This study
p5899	pFL44L	2 μm *URA3 MSN2*	This study
p5900	pFL44L	2 μm *URA3 BAP2*	This study
p5901	pFL44L	2 μm *URA3 AAH1*	This study
p5902	pFL44L	2 μm *URA3 HPT1*	This study
P6026	pFL44L	2 μm *URA3 APT2 DOT1*	This study

Figure 1

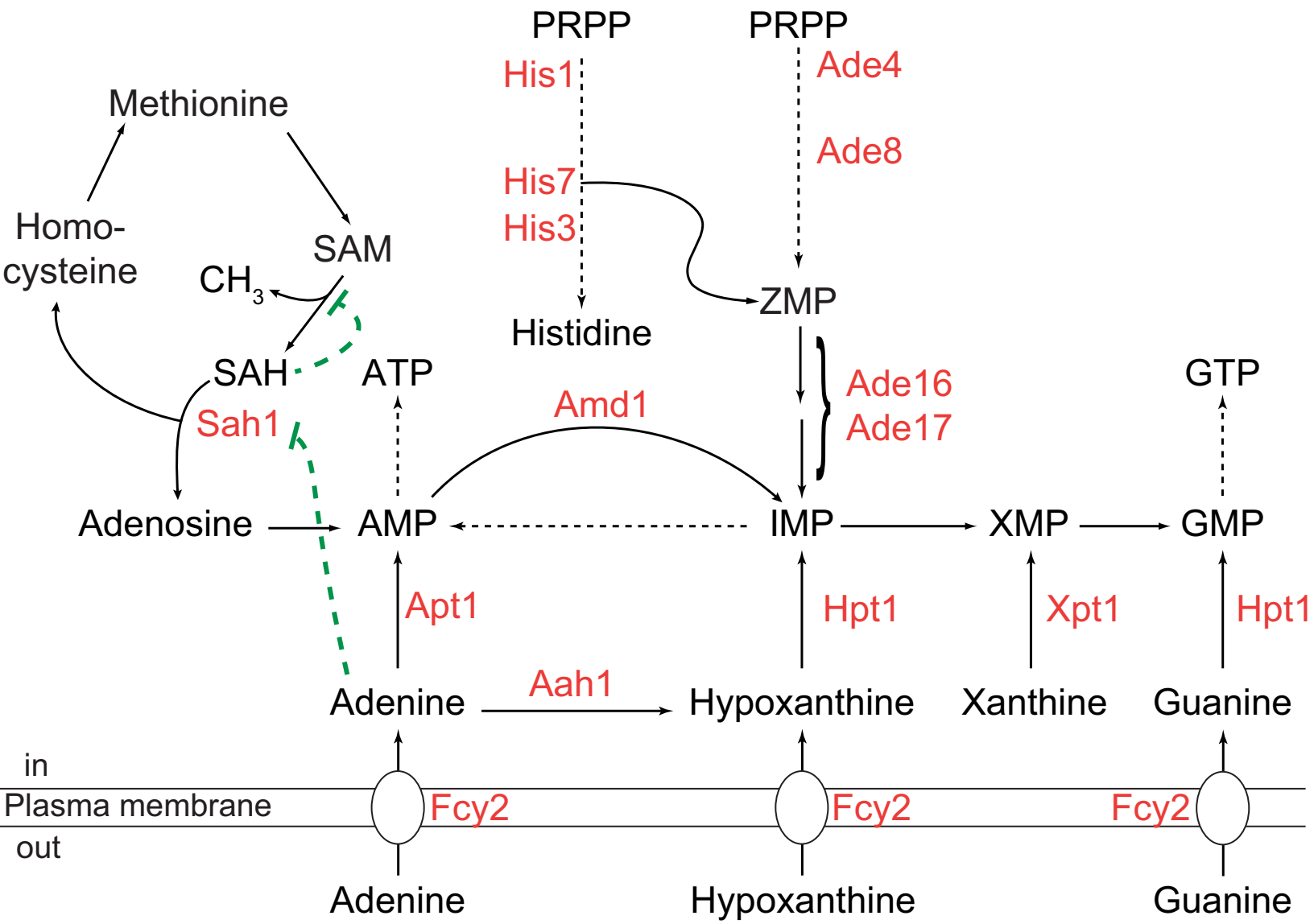

Saint-Marc *et al*
Figure 1

Figure 2

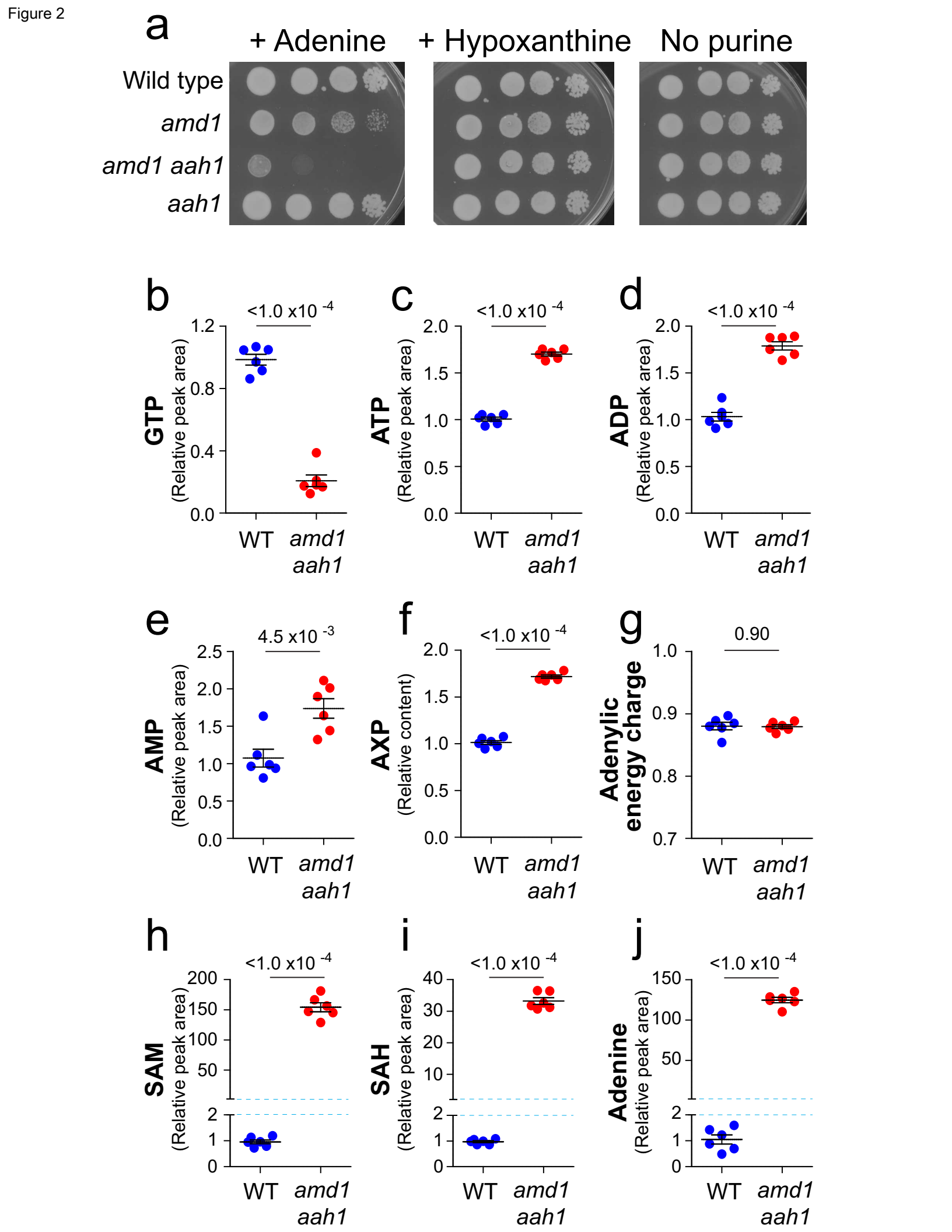
a
+ Adenine
+ Hypoxanthine
No purine
Wild type
amd1
amd1 aah1
aah1
b
GTP
(Relative peak area)
<1.0 x10 -4
WT
amd1 aah1
c
ATP
(Relative peak area)
<1.0 x10 -4
d
ADP
(Relative peak area)
<1.0 x10 -4
e
AMP
(Relative peak area)
4.5 x10 -3
f
AXP
(Relative content)
<1.0 x10 -4
g
Adenylic energy charge
0.90
h
SAM
(Relative peak area)
<1.0 x10 -4
i
SAH
(Relative peak area)
<1.0 x10 -4
j
Adenine
(Relative peak area)
<1.0 x10 -4

Figure 3

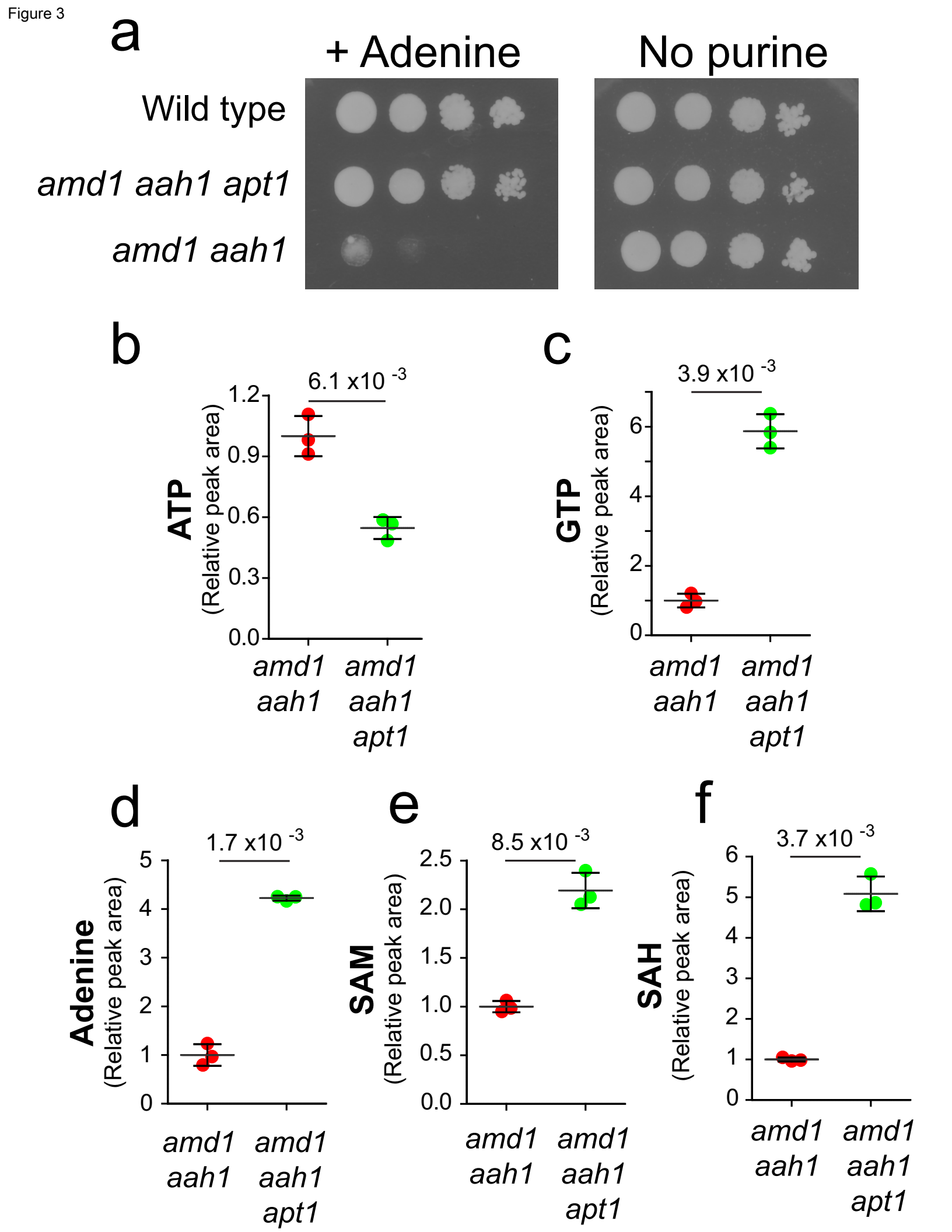
a
+ Adenine
No purine
Wild type
amd1 aah1 apt1
amd1 aah1
b
6.1 x10 -3
ATP
(Relative peak area)
1.2
0.9
0.6
0.3
0.0
amd1 aah1
amd1 aah1 apt1
c
3.9 x10 -3
GTP
(Relative peak area)
6
4
2
0
amd1 aah1
amd1 aah1 apt1
d
1.7 x10 -3
Adenine
(Relative peak area)
5
4
3
2
1
0
amd1 aah1
amd1 aah1 apt1
e
8.5 x10 -3
SAM
(Relative peak area)
2.5
2.0
1.5
1.0
0.5
0.0
amd1 aah1
amd1 aah1 apt1
f
3.7 x10 -3
SAH
(Relative peak area)
6
5
4
3
2
1
0
amd1 aah1
amd1 aah1 apt1

Figure 4

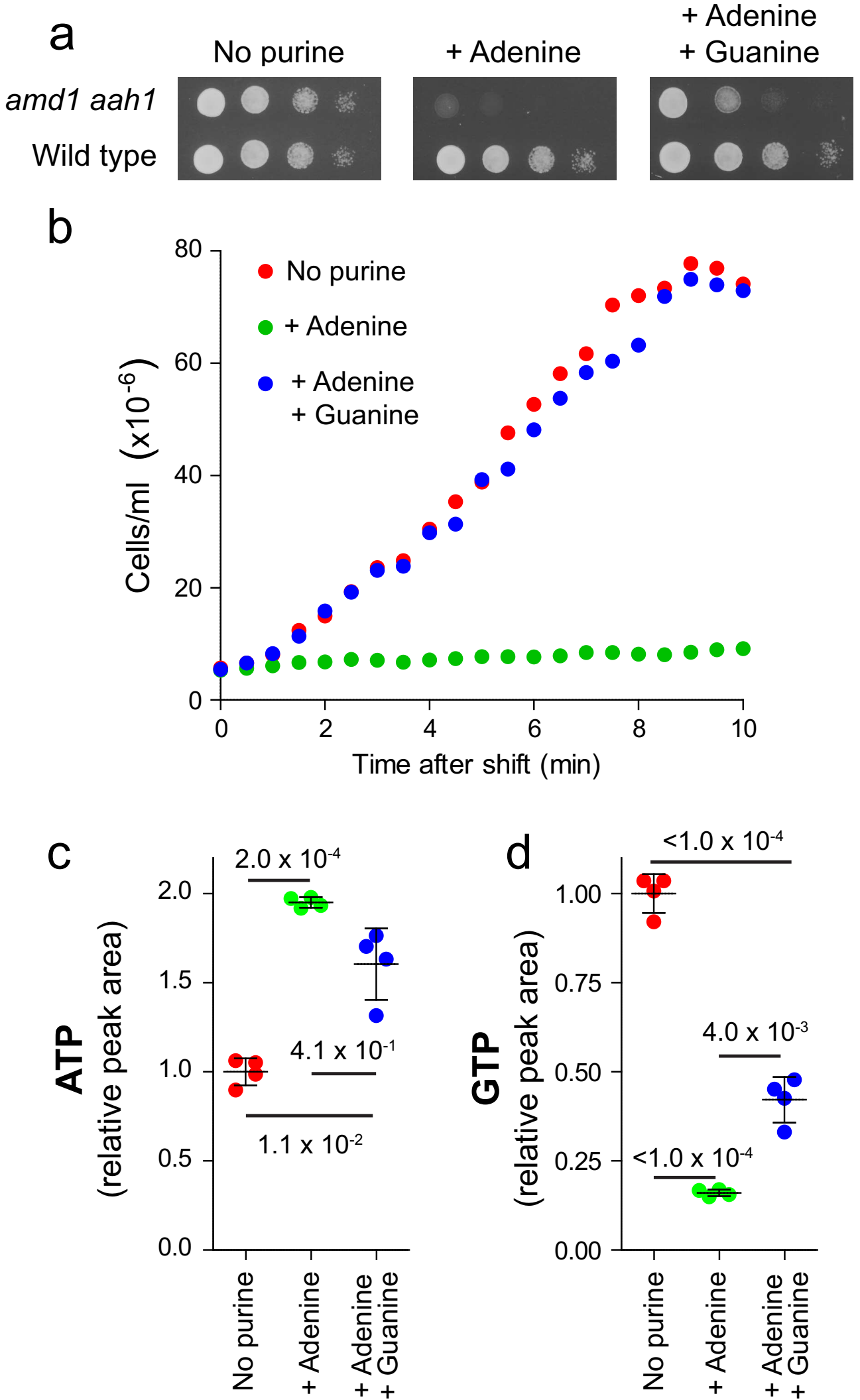
a
No purine
+ Adenine
+ Adenine
+ Guanine
amd1 aah1
Wild type
b
No purine
+ Adenine
+ Adenine
+ Guanine
Cells/ml (x10-6)
Time after shift (min)
c
ATP
(relative peak area)
2.0 x 10-4
4.1 x 10-1
1.1 x 10-2
No purine
+ Adenine
+ Adenine + Guanine
d
GTP
(relative peak area)
<1.0 x 10-4
4.0 x 10-3
<1.0 x 10-4
No purine
+ Adenine
+ Adenine + Guanine

Figure 5

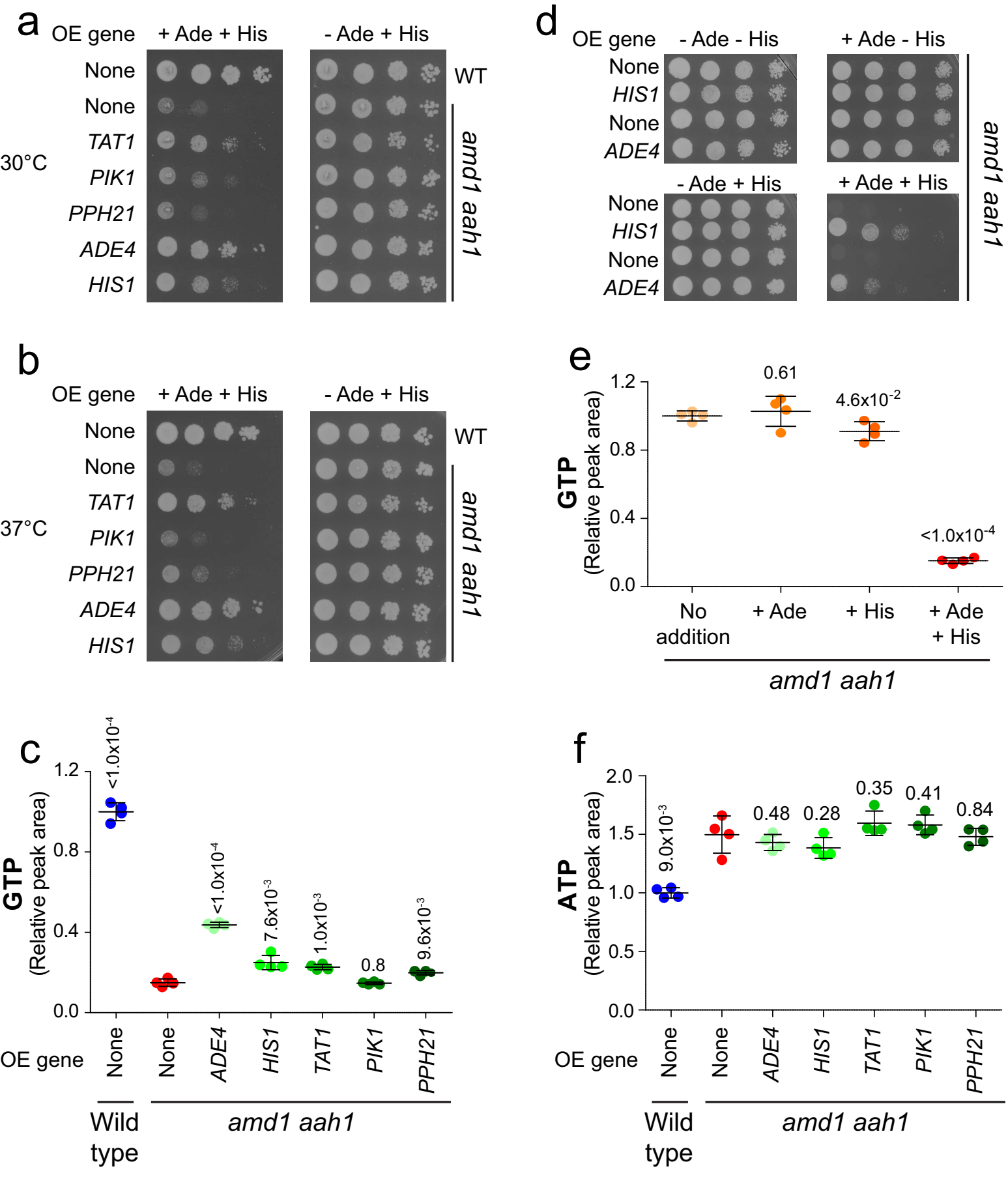
a
OE gene
+ Ade + His
- Ade + His
None
None
TAT1
PIK1
PPH21
ADE4
HIS1
30°C
WT
amd1 aah1
b
37°C
c
GTP
(Relative peak area)
<1.0x10-4
<1.0x10-4
7.6x10-3
1.0x10-3
0.8
9.6x10-3
Wild type
amd1 aah1
d
- Ade - His
+ Ade - His
- Ade + His
+ Ade + His
e
0.61
4.6x10-2
<1.0x10-4
No addition
+ Ade
+ His
+ Ade + His
f
ATP
9.0x10-3
0.48
0.28
0.35
0.41
0.84

Figure 6

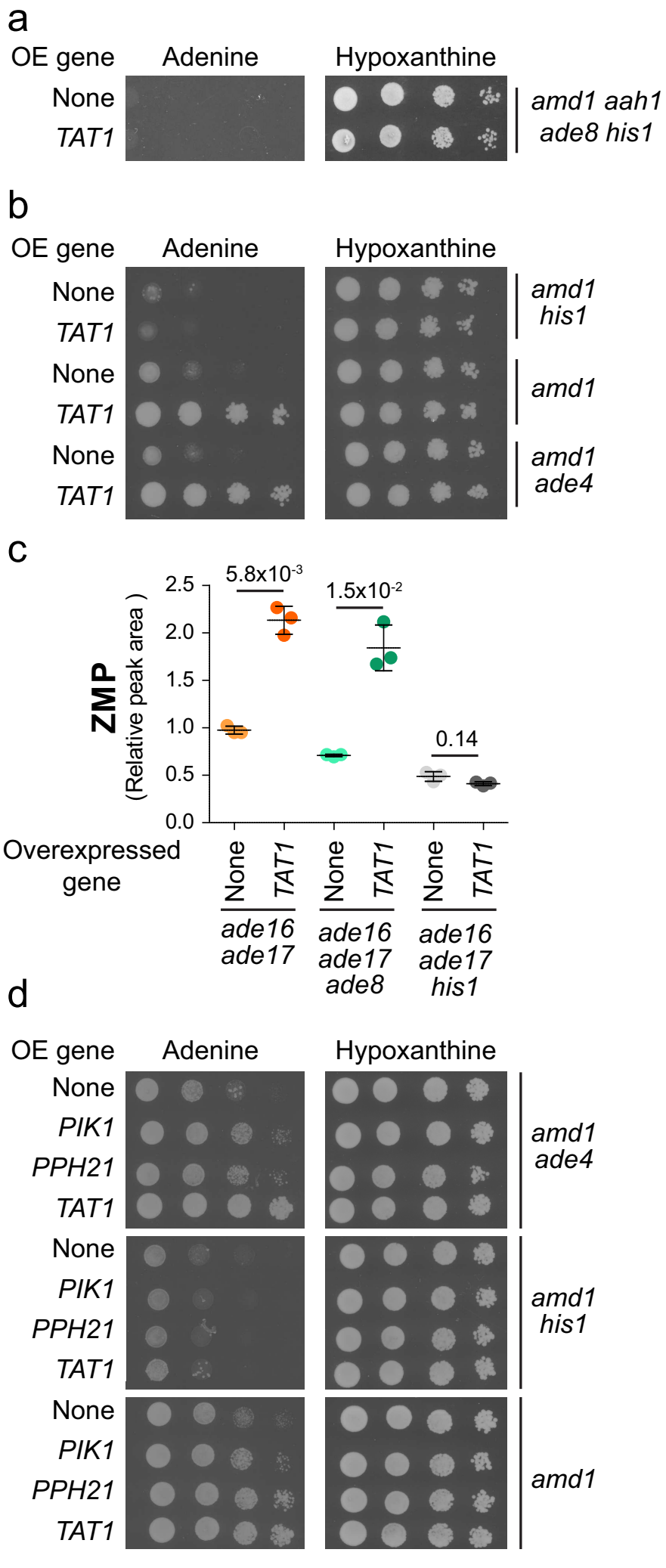
a
OE gene
Adenine
Hypoxanthine
None
TAT1
amd1 aah1
ade8 his1
b
OE gene
Adenine
Hypoxanthine
None
TAT1
amd1
his1
None
TAT1
amd1
None
TAT1
amd1
ade4
c
ZMP
(Relative peak area)
2.5
2.0
1.5
1.0
0.5
0.0
5.8x10-3
1.5x10-2
0.14
Overexpressed gene
None
TAT1
ade16
ade17
ade16
ade17
ade8
ade16
ade17
his1
d
OE gene
Adenine
Hypoxanthine
None
PIK1
PPH21
TAT1
amd1
ade4
None
PIK1
PPH21
TAT1
amd1
his1
None
PIK1
PPH21
TAT1
amd1

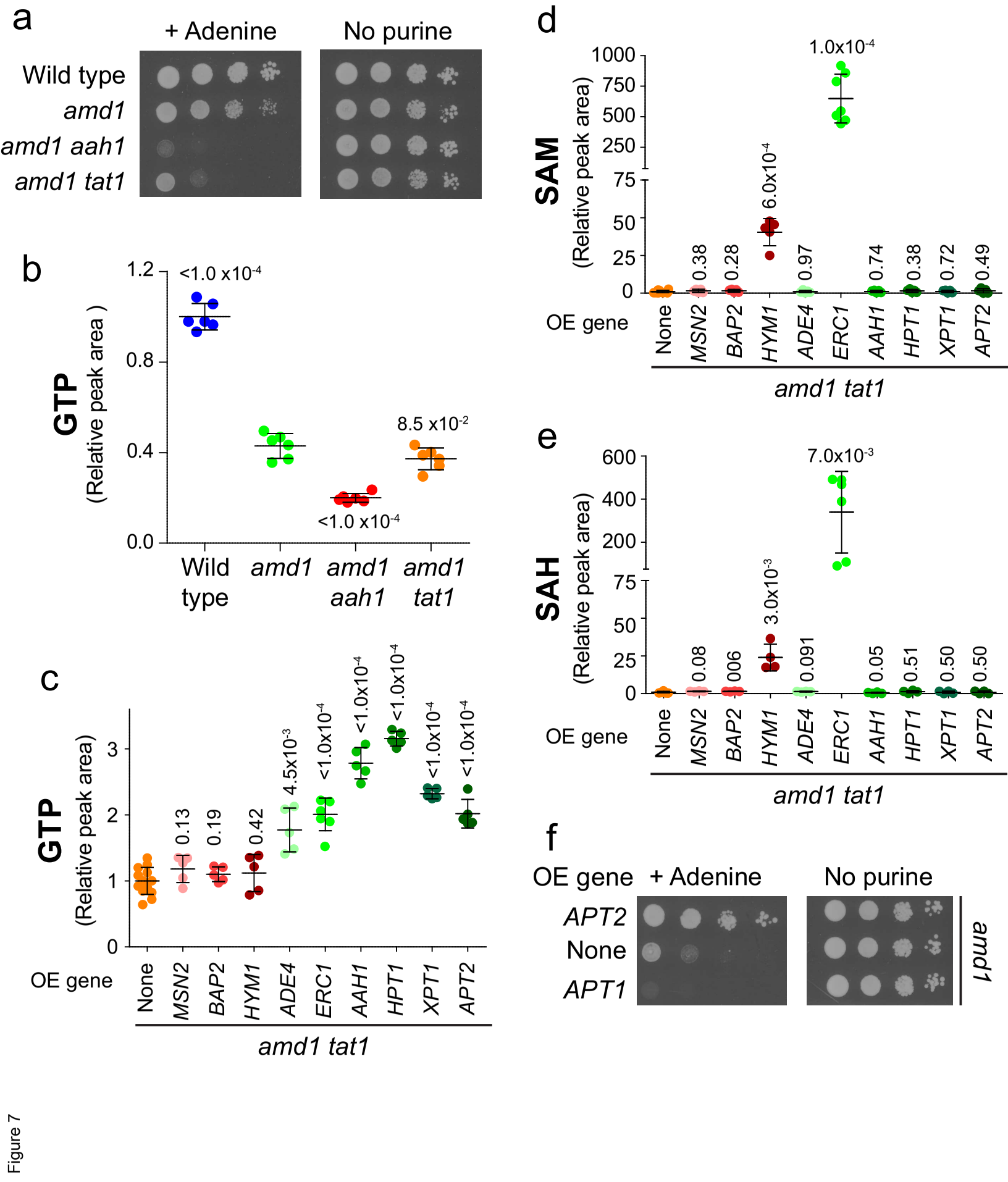
a
+ Adenine
No purine
Wild type
amd1
amd1 aah1
amd1 tat1
b
GTP
(Relative peak area)
1.2
0.8
0.4
0.0
<1.0 x10-4
8.5 x10-2
<1.0 x10-4
Wild type
amd1
amd1 aah1
amd1 tat1
c
GTP
(Relative peak area)
3
2
1
0
0.13
0.19
0.42
4.5x10-3
<1.0x10-4
<1.0x10-4
<1.0x10-4
<1.0x10-4
<1.0x10-4
OE gene
None
MSN2
BAP2
HYM1
ADE4
ERC1
AAH1
HPT1
XPT1
APT2
amd1 tat1
d
SAM
(Relative peak area)
1000
750
500
250
75
50
25
0
1.0x10-4
6.0x10-4
0.38
0.28
0.97
0.74
0.38
0.72
0.49
OE gene
None
MSN2
BAP2
HYM1
ADE4
ERC1
AAH1
HPT1
XPT1
APT2
amd1 tat1
e
SAH
(Relative peak area)
600
400
200
75
50
25
0
7.0x10-3
3.0x10-3
0.08
006
0.091
0.05
0.51
0.50
0.50
OE gene
None
MSN2
BAP2
HYM1
ADE4
ERC1
AAH1
HPT1
XPT1
APT2
amd1 tat1
f
OE gene
+ Adenine
No purine
APT2
None
APT1
amd1

Figure 7

Click here to access/download
Supplementary Material
Saint Marc et al Supplemental data.pdf